Journal of Cellular Biochemistry 103:1938–1951 (2008)

Opposing Effects of Glucocorticoids and Wnt Signaling on Krox20 and Mineral Deposition in Osteoblast Cultures

Nathalie Leclerc,[1] Tommy Noh,[1] Jon Cogan,[1] Dilan B. Samarawickrama,[1] Elisheva Smith,[2] and Baruch Frenkel[1,2]*

[1]Department of Biochemistry & Molecular Biology, Institute for Genetic Medicine, Keck School of Medicine at the University of Southern California, Los Angeles, California 90033
[2]Department of Orthopaedic Surgery, Institute for Genetic Medicine, Keck School of Medicine at the University of Southern California, Los Angeles, California 90033

Abstract Krox20 is expressed in osteoblasts and chondrocytes, and is required for trabecular bone formation during embryogenesis. Here we show by RT-qPCR and Western blot analysis that Krox20 is up-regulated during late stages of osteoblast differentiation in culture. Glucocorticoids (GCs) rapidly inhibit the expression of Krox20 as well its co-activator, HCF-1, resulting in inhibition of the Osteocalcin Krox20-binding Enhancer (OKE). GCs also inhibit expression of EGR1, EGR3, and EGR4. OKE activity, which is dependent on the presence of Runx2, was independent of the osteocalcin promoter Runx2 binding site. In contrast to GCs, activation of the Wnt, but not the BMP or the PTH signaling pathways, stimulated Krox20 expression as well as activity of the OKE. GC-mediated suppression of Krox20 expression was compromised, albeit not completely, in the presence of DKK1, suggesting that the inhibition occurs in both Wnt-dependent and Wnt-independent manners. Furthermore, Wnt3A partially rescued Krox20 expression in GC-arrested osteoblast cultures and this was accompanied by rescue of mineralization. These findings are consistent with a role for Krox20 in osteoblast function and suggest that this transcription factor may contribute to the opposing effects of GCs and Wnt signaling on bone formation. J. Cell. Biochem. 103: 1938–1951, 2008.

Key words: early growth response genes; Krox20; glucocorticoids; Wnt signaling; osteoblast; mineralization

The family of early growth response (EGR) genes consists of four members, EGR1/Krox24, EGR2/Krox20, EGR3, and EGR4 (reviewed in Gashler and Sukhatme [1995]). Their expression is rapidly induced by serum and growth factors, such as nerve growth factor, epidermal growth factor, and platelet-derived growth factor [Milbrandt, 1987; Christy et al., 1988; Lemaire et al., 1988]. The four EGR proteins are transcription factors with a highly conserved DNA-binding domain composed of three zinc-fingers, which recognize G:C-rich DNA motifs [Chavrier et al., 1988; Gashler and Sukhatme, 1995; Swirnoff and Milbrandt, 1995; O'Donovan et al., 1999] in the promoters of target genes such as Hox-1.4 [Chavrier et al., 1990], Hoxa-2 and Hoxb-2 [Nonchev et al., 1996], thymidine kinase [Chavrier et al., 1990; Molnar et al., 1994], and synapsin I and II [Petersohn et al., 1995; Thiel and Cibelli, 2002]. The transactivation activity of EGR factors is modulated by co-activators such as HCF-1 [Luciano and Wilson, 2003], and co-repressors such as NAB1 [Russo et al., 1995], NAB2 [Svaren et al., 1996], and Ddx20 [Gillian and Svaren, 2004].

Whereas early studies highlighted the role of EGR genes in cell proliferation [Lemaire et al., 1988], more recent investigations using knock-out mice assigned roles for the EGR genes in specific organ systems (reviewed in O'Donovan et al. [1999]). EGR1-deficient mice present endocrine abnormalities, in particular a marked reduction in pituitary luteinizing hormone and lack of luteinizing hormone receptor expression in ovaries, resulting in male and

*Correspondence to: Baruch Frenkel, Institute for Genetic Medicine, University of Southern California Keck School of Medicine, 2250 Alcazar Street, CSC/IGM240, Los Angeles, CA 90033. E-mail: frenkel@usc.edu

Received 3 April 2007; Accepted 27 August 2007
DOI 10.1002/jcb.21587

female infertility [Lee et al., 1996; Topilko et al., 1998]. EGR2 knockout mice have severe abnormalities in hindbrain development [Wilkinson et al., 1989; Schneider-Maunoury et al., 1993] and impaired peripheral nerve myelination [Topilko et al., 1994]. Mice lacking EGR3 display severe motor abnormalities due to the absence of muscle spindles [Tourtellotte and Milbrandt, 1998], and deficiency in EGR4 dramatically alters sperm production and maturation resulting in male infertility [Tourtellotte et al., 1999].

Little is known about the role of EGRs in bone. EGR1-deficient mice have low bone mass, attributable to hypogonadism and increased bone turnover [Cenci et al., 2000]. Additionally, retinoic acid and prostaglandin E2, which stimulate osteoblastic cell proliferation and differentiation, increase the expression of EGR1 [Suva et al., 1991; Fang et al., 1996]. EGR2 is expressed in long bone chondrocytes and osteoblasts [Levi et al., 1996] and EGR2 deficiency results in a severe defect in trabecular bone formation [Levi et al., 1996]. Moreover, EGR2 binds an enhancer element at the Osteocalcin (OC) promoter, which is operative in osteoblasts as well as fibroblasts that forcibly express Runx2 [Leclerc et al., 2005].

The Wnt signaling pathway plays a critical role in bone mass control. Inactivating mutations in the Wnt co-receptor *LRP5* cause osteoporosis in humans [Gong et al., 2001] and *LRP5*-deficient mice also have low bone mass [Kato et al., 2002]. Furthermore, mutations in *LRP5* that increase Wnt signaling are associated with high bone mass in both humans and mice [Boyden et al., 2002; Little et al., 2002; Babij et al., 2003]. Alterations in other components of the Wnt signaling pathway also affect bone mass (reviewed in Glass and Karsenty [2006]). Several studies suggest that the Wnt signaling pathway controls bone mass by stimulating osteoblast proliferation, survival, and differentiation (reviewed in Westendorf et al. [2004] and Glass and Karsenty [2006]). However, Wnt target genes that mediate its bone anabolic effect are largely unknown.

Glucocorticoids (GCs) are anti-inflammatory drugs widely prescribed for the management of rheumatoid arthritis, lupus erythematosus, asthma, cancer, and organ transplantation. However, the beneficial properties of GCs are accompanied by rapid bone loss and increased risk of fractures [Van Staa et al., 2000]. The primary cause of long-term GC-induced osteoporosis (GIO) is the inhibition of bone formation due to impaired osteoblast function (reviewed in Canalis [2005] and Mazziotti et al. [2006]). GCs inhibit Wnt signaling in osteoblasts by activating glycogen synthase kinase 3β [Smith et al., 2002], inhibiting the transcriptional activity of LEF/TCF [Smith and Frenkel, 2005] and enhancing the expression of Wnt inhibitors [Ohnaka et al., 2004; Ohnaka et al., 2005; Wang et al., 2005]. GCs also inhibit the expression of EGR genes in osteoblasts [Leclerc et al., 2004, 2005] as well as immune cells [Kharbanda et al., 1991; Hass et al., 1992; Mittelstadt and Ashwell, 2001].

In the present study, we pursued a possible link between GCs, Wnt signaling and EGR2/Krox20 in osteoblasts. We show that Krox20 is stimulated by the Wnt signaling pathway and is rapidly inhibited by GCs partly via inhibition of the Wnt pathway. Furthermore, Wnt3A partially reverses the inhibitory effect of GCs on both Krox20 expression and mineral deposition.

MATERIALS AND METHODS

Cell Culture

MC3T3-E1 cells, isolated based on their robust mineralization and the strong inhibitory effect of dexamethasone (DEX) [Smith et al., 2000], were plated in 12-well plates for luciferase assays and alizarin red staining, and in 6-well plates for mRNA expression analysis. Newborn mouse calvarial osteoblast (NeMCO) cultures were prepared from one day-old pups. The parietal bones were cleaned from all sutures and subjected to sequential digestion with 1% Collagenase P (Roche Applied Science, Indianapolis, IN) and 0.25% Trypsin (Invitrogen, Carlsbad, CA) in phosphate buffer saline. The first and second digestions were discarded and cells obtained from the last digestion were plated in 6-well plates for mRNA expression analysis and in 12-well plates for alizarin red staining. Both MC3T3-E1 cells and NeMCOs were plated at a density of 8,000 cells/cm^2 and maintained in α-minimum essential medium (Invitrogen) supplemented with 10% fetal bovine serum (Invitrogen). When indicated, cells were treated with DEX (Sigma), recombinant mouse Wnt3A (rmWnt3A, R&D Systems, Minneapolis, MN), lithium chloride (LiCl, Sigma), potassium chloride (KCl, Sigma), recombinant human BMP2 (rhBMP2, Wyeth Research,

Cambridge, MA), recombinant human DKK1 (rhDKK1, R&D Systems), and rat PTH(1-34) (Bachem, Torrance, CA). In short-term experiments, reagents were gently added to the cultures drop wise without feeding, to minimize response of EGRs to mitogenic stimuli and/or fluid shear stress. To facilitate osteogenic differentiation, the culture medium was supplemented with 50 μg/ml ascorbic acid (Sigma) and 10 mM β-glycerophosphate (Sigma) when cultures reached confluency.

Plasmid Construction

To construct OKE_3-147-OC-Runx2m-Luc, we initially mutated the OSE2 site in −147-OC-Luc [Ducy and Karsenty, 1995]. The CAACCACA sequence (core Runx2 motif underlined) was replaced by *CtgCag*CA, thus generating a unique *Pst*I site (italicized). The forward primer used for PCR mutagenesis was 5′-GCCCAGGTACCTGCAATCACCtgCagCAGCATCCTTTGGG-3′. The reverse primer, which overlaps the transcription start site and contains a *Sal*I site, was 5′-CTGTGGTCGACTTGTCTGTTCTGC-3′. The resultant construct, −147-OC-Runx2m-Luc was digested with *Pst*I and *Kpn*I, the latter recognizing a restriction site in the vector immediately upstream of the *Pst*I site. A PCR fragment containing three copies of the OKE was amplified from the OKE_3-147-OC-Luc [Leclerc et al., 2005] using a forward primer containing a *Kpn*I restriction site (5′-CCCCGGGTACCGAGCCTTGCCCAGGCAAG-3′) and a reverse primer containing a *Pst*I restriction site (5′-TGCTGCTGCAGGTGATTGCAGGACCTCGAG-3′). The PCR product was digested with *Kpn*I and *Pst*I, and ligated with the *Kpn*I/*Pst*I-digested −147-OC-Runx2m-Luc. Correct construction of both plasmids was verified by restriction digestions and sequencing.

Transfection and Luciferase Assays

MC3T3-E1 cells were transiently transfected using the Lipofectamin LTX reagent (Invitrogen) according to the manufacturer's instructions or using the calcium phosphate co-precipitation method as previously described [Leclerc et al., 2005]. Stable transfection of MC3T3-E1 cells was performed essentially as described previously [Frenkel et al., 1996] using the calcium phosphate co-precipitation method and hygromycin (100 ng/ml) as the selection drug. Luciferase activity was measured using the Luciferase Assay System kit (Promega, Madison, WI).

RNA Analysis

Total RNA was isolated using Aurum Total RNA kit (Bio-Rad, Hercules, CA) following the manufacturer's recommendations. One microgram of total RNA was reverse-transcribed (Invitrogen) and the cDNA was subjected to real-time PCR amplification (RT-qPCR) using IQ SYBR Green (Bio-Rad), unless otherwise stated. The following forward (F) and reverse (R) PCR primers were designed using the Primer3 program (http://frodo.wi.mit.edu/cgi-bin/primer3/primer3_www.cgi): EGR1/Krox24: F 5′-CCCTGACTATCTGTTTCC-3′, R 5′-TCTGCTTTCTTGTCCTTC3′; EGR2/Krox20: F 5′-ATCACAGGCAGGAGAGAGTC-3′, R 5′-AGGCTGTGGTTGAAGCTG-3′; EGR3: F 5′-CCTCCTTATTCCAACTGC-3′, R 5′-AGAACTC-ACAGGCAAAGG-3′; EGR4: F 5′-ACAGCGGCAGCTTCTTCATC-3′, R 5′-GACCTTGGTCCCTACTGCAGAG-3′; HCF-1: F 5′-ATCACTT-CCCCAAGAGCTGA-3′, R 5′-CTCAGTGGGAAGATGGTGCT-3′; Ddx20: F 5′-GGCTCCCACAAGAGAAATTG-3′, R 5′-TGCCAACATCT-GCTTACTCG-3′; NAB1: F 5′-CTGCAGCAGGAGAGGAGACT-3′, R 5′-GGACTTGGCCTCACTGGAG-3′; NAB2: F 5′-GAAATCCAGCA-GCCTCCTC-3′, R 5′-CCACACGATCATGGGAGAC-3′; rpL10A: F 5′-CGCCGCAAGTTTCTGGAGAC-3′, R 5′-CTTGCCAGCCTTGTTTAG-GC-3′.

Western Blot Analysis

NeMCOs were washed, collected and centrifuged in phosphate-buffered saline, and pellets were resuspended in 1.5 packed cells volume of lysis buffer (60 mM Tris−Cl pH 6.8, 2% SDS). Lysates were boiled for 5 min and further dissociated by several passes through 23-gauge needles, followed by centrifugation at 16,000 rpm for 30 min at 4°C to remove cell debris. The protein concentration was determined using the micro BCA Protein Assay kit (Pierce, Rockford, IL) and 20 μg were subjected to electrophoresis in a 10% polyacrylamide denaturating gel. Equal loading was verified by Coomassie staining and Krox20 was detected as described previously [Leclerc et al., 2004].

Inhibition of Translation

MC3T3-E1 cells were pre-treated for 30 min with 10 μM of the translational inhibitor

cycloheximide (CHX), and then 1 μM DEX was added to the cultures for 4 h. Total RNA was isolated from the cells using Triazol reagent (Invitrogen) and cDNA was synthetized using the SuperScript III First Strand Synthesis System (Invitrogen). Following DNAse I treatment, EGR2/Krox20 and ribosomal protein L10A (rpL10A) mRNA levels were assessed using PCR, electrophoresis on 1% agarose gel and densitometric analysis using the Gene Genius Bio Imaging System (Syngene).

Histological Assessment of Calcium Deposition

Culture wells were washed once with cold phosphate-buffer saline and fixed for 1 h at 4°C in 70% ethanol. Calcium deposits were stained for 10 min at room temperature with filtered alizarin red solution (40 mM, pH 4.2). Non-specific staining was removed by several washes in water.

Statistical Analysis

Mean values from quantitative assays were compared by the unpaired *t*-test using GraphPad Instat version 3.0 for PC. Differences were considered significant when $P \leq 0.05$.

RESULTS

Krox20 is Up-Regulated During Terminal Osteoblast Differentiation and Repressed by GCs

Microarray analysis of GC-arrested MC3T3-E1 osteoblastic cells disclosed strong repression of Krox20 [Leclerc et al., 2004], a gene previously implicated in osteogenesis [Levi et al., 1996]. We initially followed Krox20 expression as a function of time during development of the osteoblast phenotype in MC3T3-E1 cultures. As shown in Figure 1A, Krox20 mRNA progressively increased, reaching on Day 12 levels that were 1.6-fold higher than those observed on Day 3. Treatment with 1 μM DEX, which

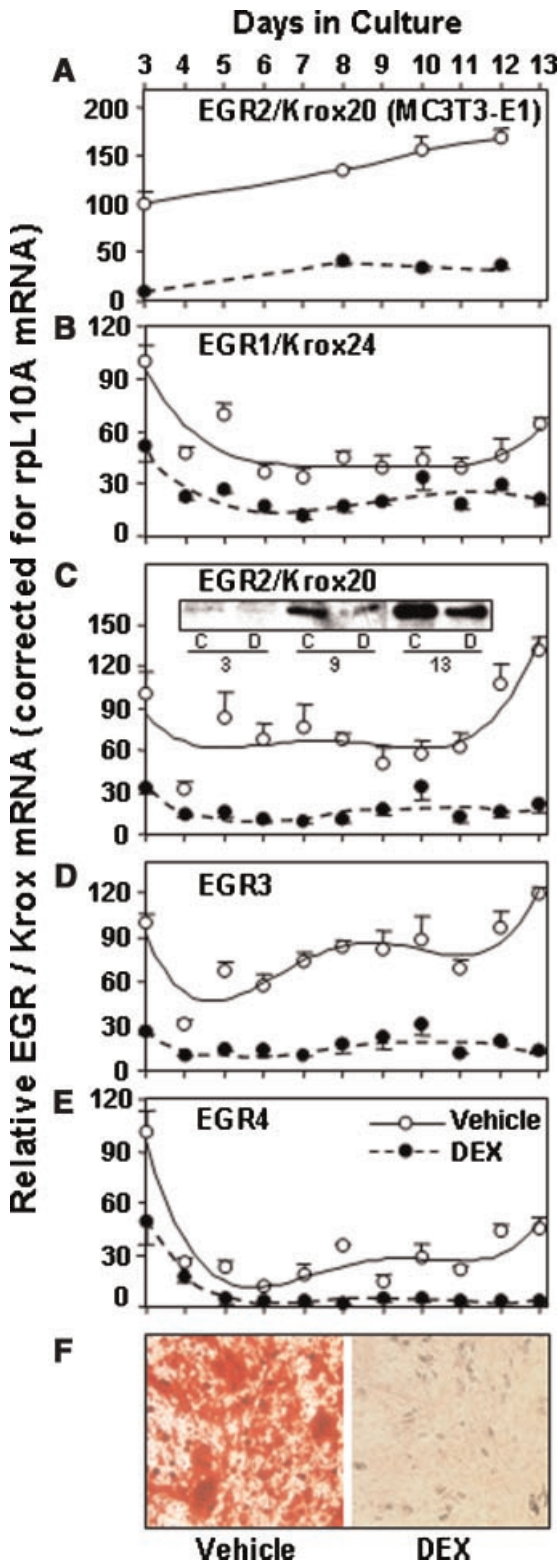

Fig. 1. Basal and GC-regulated expression of EGR genes during osteoblast differentiation. **A**–**E**: Cells were plated and treated, commencing on Day 2, with osteogenic medium containing either 1 μM DEX (*closed circles*) or ethanol vehicle (*open circles*). Expression of the indicated EGR genes was measured by RT-qPCR between Days 3 and 13 of MC3T3-E1 (A) and primary NeMCO (B–E) cultures. Results were corrected for the respective ribosomal protein L10A (rpL10A) mRNA levels, which themselves did not significantly change in response to culture progression or DEX treatment. Data (mean ± SD, n = 3) is normalized to the Day-3 control levels, defined in each case as 100. Inset in **Panel C** shows Western analysis of Krox20 in NeMCO cultures treated as above and harvested on Days 3, 9 and 13. **F**: NeMCO cultures were treated as above with DEX (*right*) or vehicle (*left*). Micrographs show alizarin red staining of fully differentiated cultures (100×). [Color figure can be viewed in the online issue, which is available at www.interscience.wiley.com.]

strongly suppresses differentiation [Smith et al., 2000; Leclerc et al., 2004] inhibited Krox20 expression at each of the time points tested (Fig. 1A). Notably, DEX inhibited Krox20 expression even in pre-confluent uncommitted cultures, when it does not inhibit cell cycle progression [Smith et al., 2000] (data not shown). Similar to the MC3T3-E1 model, analysis of primary Newborn Mouse Calvarial Osteoblast (NeMCO) cultures demonstrated a differentiation-related up-regulation of Krox20 expression, with a 2.1-fold increase in Krox20 mRNA between Days 11 and 13 (Fig. 1C), concomitant with mineralization of the extracellular matrix (data not shown). DEX significantly inhibited Krox20 mRNA expression in NeMCO cultures at every time point tested between Days 3 and 13. Western analysis confirmed a progressive increase in Krox20 protein levels during development of the osteoblast phenotype, with DEX displaying an inhibitory effect at all stages. These results are consistent with a role for Krox20 in terminal osteoblast differentiation.

We also followed expression of the other members of the EGR gene family in NeMCO cultures. Interestingly, each of EGR1, 3, and 4 also displayed a differentiation-related increase in gene expression, amounting to 1.6-, 1.7-, and 2.1-fold, respectively, between Days 11 and 13 (Fig. 1B,D,E). However, EGR1 and EGR4 mRNA levels did not reach their respective Day-3 levels. The expression pattern of all EGR genes also shared a decrease during the first days of culture (Fig. 1B–E), possibly related to the down-regulation of proliferation. DEX strongly inhibited expression of all EGR family members at every time point tested (Fig. 1B–E), paralleling the inhibitory effect of GCs on both osteoblast proliferation and differentiation. Figure 1F demonstrates, by alizarin red staining, the inhibitory effect of DEX on calcium deposition in NEMCO cultures.

DEX Rapidly Inhibits Krox20 mRNA Expression

The up-regulation of Krox20 during terminal osteoblast differentiation, along with the in vivo Krox20 knockout bone phenotype [Levi et al., 1996], suggest a role for this gene in osteoblastogenesis, abrogation of which could potentially contribute to GC-induced osteoporosis (GIO).

To investigate whether GCs inhibit Krox20 expression in osteoblasts directly, we initially measured Krox20 mRNA in MC3T3-E1 cultures 1, 2, 4, and 8 h after addition of either 1 μM DEX or ethanol vehicle. In response to the addition of vehicle, Krox20 mRNA increased by 46% within 1 h, followed by a time-dependent decrease to 14% of the initial level at 8 h (Fig. 2A). The other three EGR genes responded to the addition of vehicle in a similar manner (data not shown). The up-regulation of the EGR mRNAs observed in the control cultures, presumably a response to physical manipulation (see Materials and Methods Section), was not observed in the DEX-treated cultures. In these cultures, DEX significantly inhibited the expression of the EGRs at all time points tested. Specifically, as shown in Figure 2A for Krox20, the transcript level was immediately and strongly repressed, reaching within 1 h 53% of the initial level, or 32% of the level observed in the control cultures. At this time point, DEX repressed all EGR mRNAs (Fig. 2A, inset). Overall, the DEX-mediated inhibition of EGR3 followed a pattern similar to that of Krox20, and EGR4 was the least inhibited (Fig. 2A, inset). In a subsequent, shorter time course experiment, DEX significantly inhibited Krox20 expression to 50% the initial control level within as little as 15 min (Fig. 2B). This rapid inhibition suggests a direct effect of GCs on Krox20 expression.

To confirm that the inhibition of Krox20 by GCs does not require de novo protein synthesis, and to test whether such a direct effect persists beyond a few minutes, we measured Krox20 expression in cultures treated with DEX for 4 h in the presence of the translational inhibitor cycloheximide (CHX). As shown in Figure 2C, DEX significantly decreased Krox20 mRNA in the presence of CHX, suggesting a direct effect. However, the inhibition in the presence of CHX amounted to only 28%, much less than the 81% inhibition measured in the absence of CHX (Fig. 2C). The compromised effect of GCs in the presence of CHX may suggest that their long-term (hours) inhibitory effect is in part indirect, requiring new protein synthesis. Alternatively, CHX could stabilize Krox20 mRNA, partially masking a stronger, direct effect of GCs on Krox20 transcription.

GCs Modulate the Expression of Krox20 Co-Regulators

We next tested whether Krox20 co-activators and co-repressors were also regulated by DEX. Unlike Krox20 itself (Fig. 2A), expression of its co-regulators was not as sensitive to physical

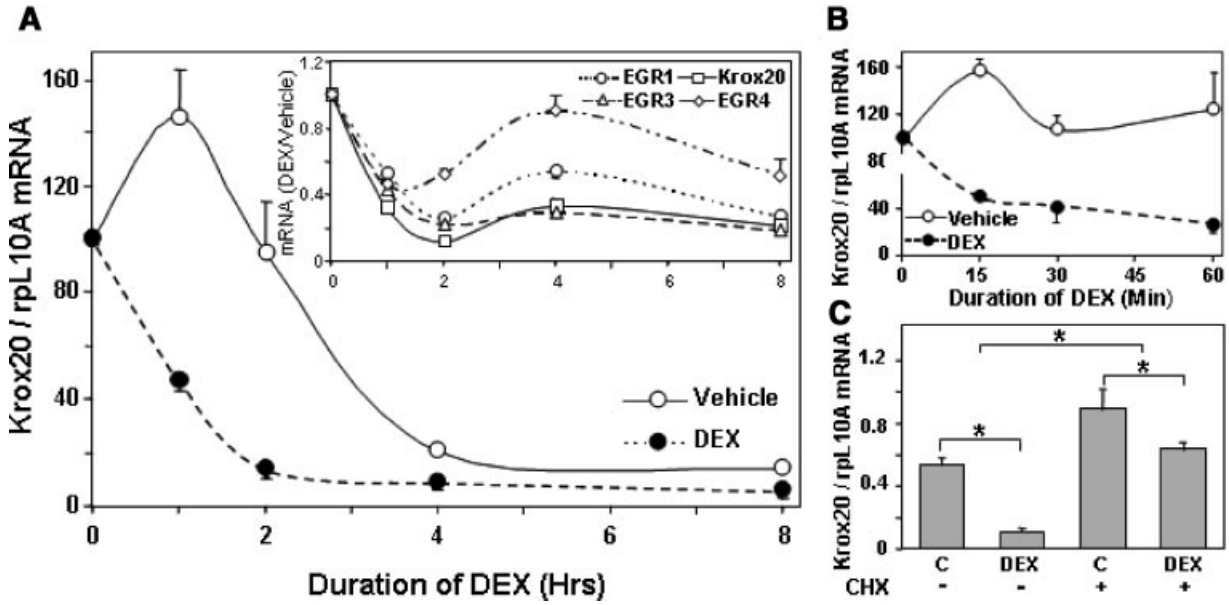

Fig. 2. DEX inhibits Krox20 mRNA expression rapidly and directly. **A**: Krox20 mRNA was measured by RT-qPCR in Day-4 MC3T3-E1 cultures that were treated for 1, 2, 4, and 8 h with either 1 μM DEX (*closed circles*) or vehicle (*open circles*). Treatment was delivered without medium change. *Inset* shows the inhibitory effect at each time point as the DEX/Vehicle ratio for Krox20 as well as the other EGR mRNAs measured in the same samples. **B**: Krox20 mRNA was measured as in **Panel A** after shorter (up to 1-h) treatment periods. **C**: MC3T3-E1 cultures were pre-incubated for 30 min with 10 μM cycloheximide, followed by 4 h of treatment with either 1 μM DEX or vehicle. Krox20 mRNA was measured as described in Materials and Methods Section and corrected for rpL10A mRNA. Mean ± SD, n = 3; $^*P \leq 0.05$.

manipulation of the cultures, and did not significantly change after addition of vehicle (data not shown). DEX halved the expression of HCF-1, the only known Krox20 co-activator [Luciano and Wilson, 2003], within 2 h, and this effect was sustained and remained significant for the entire 24-h time course (Fig. 3). The expression of Ddx20, one of three known Krox20 co-repressors [Gillian and Svaren, 2004], was stimulated by 50% after 4 h of DEX treatment, but then decreased to 60–70% of the control level (Fig. 3). The EGR co-repressors NAB1 and NAB2 [Russo et al., 1995] were inhibited in a cyclical fashion. In the case of NAB2, the cyclical repression could reflect the fact that it is not only a regulator, but also a transcriptional target of Krox20 [Gillian and Svaren, 2004]. Thus, the repression of NAB2 after 2 h of DEX treatment (Fig. 3) could result from the rapid inhibition of Krox20 expression (Fig. 2A,B), while the ensuing increase in NAB2 mRNA levels could result from its negative auto-regulation. By 8 h, both NAB1 and NAB2 reached new steady state levels that were 30% and 20% lower than the respective control levels (Fig. 3). In all, the transient 50% stimulation of Ddx20 and the sustained 50% repression of HCF-1, along with the sevenfold repression of Krox20 itself (Fig. 2A), appear to be the major events contributing to the GC-mediated 50% loss in Krox20 transcriptional activity [Leclerc et al., 2005].

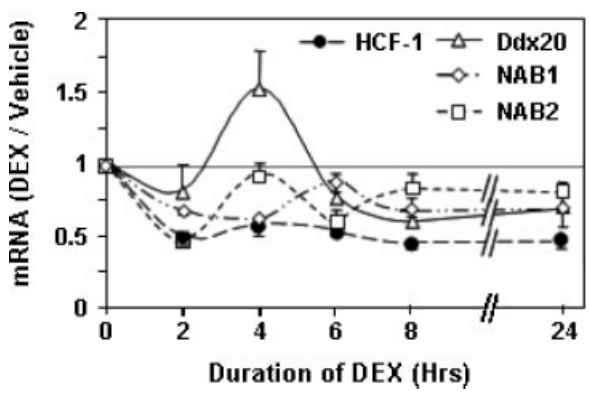

Fig. 3. DEX modulates the expression of Krox20 co-regulators. Day-4 MC3T3-E1 cultures were treated with 1 μM DEX or vehicle and the mRNAs for HCF-1, Ddx20, NAB1 and NAB2 were measured by RT-qPCR. Values were corrected for the expression of rpL10A mRNA. Results (Mean ± SD, n = 3) represent ratios of the corrected mRNA levels in the DEX-treated with respect to the control cultures.

Wnt Signaling Stimulates Krox20

Krox20 expression is linked to osteoblast differentiation (Fig. 1). Consistent with this,

activity of the recently discovered Osteocalcin Krox20-binding Enhancer (OKE), located just 11-bp upstream of the classical Runx2-binding OSE2 element [Ducy and Karsenty, 1995; Banerjee et al., 1996], was demonstrable in MC3T3-E1 osteoblastic cells and in C310T1/2 mouse embryo fibroblasts transfected with Runx2, but not in naïve C310T1/2 cells [Leclerc et al., 2005]. To explore the interaction between Krox20 and Runx2, we transfected MC3T3-E1 cells with an OKE reporter construct in which the OSE2 site was mutated. As shown in Figure 4A, OKE significantly enhanced transcription from the proximal OC promoter by 5- to 6.6-fold, regardless of whether OSE2 was mutated. Thus, although the OKE activity is dependent on Runx2 expression [Leclerc et al., 2005], it is independent of the adjacent Runx2-binding OSE2 site. Because OKE activity in MC3T3-E1 cells requires that the cultures enter a specific developmental stage [Leclerc et al., 2005], we believe that the role of Runx2 is to provide a permissive environment for the OKE activity.

Among the most important drivers of osteoblast growth and differentiation is the Wnt signaling pathway, and inhibition of the Wnt pathway by GCs plays an important role in abrogation of the osteoblast phenotype [Smith et al., 2002; Ohnaka et al., 2004; Smith and Frenkel, 2005; Wang et al., 2005]. GCs also suppress Krox20 mRNA (Figs. 1A,C and 2), and inhibit by 50% the activity of both the OKE [Leclerc et al., 2005] and the Krox reporter 4 × Egr.syn (data not shown), which contains four consensus EGR motifs [Gillian and Svaren, 2004]. We therefore examined whether the Wnt pathway regulates Krox20, initially by transfecting MC3T3-E1 cells with the Krox reporter plasmids OKE_3-147-OC-Luc (illustrated in Fig. 4A) and 4 × Egr.syn [Gillian and Svaren, 2004]. As control, MC3T3-E1 cells were also transfected with $OKEm_3$-147-OC-Luc, in which each of the three OKE sequences in OKE_3-147-OC-Luc was mutated to abolish Krox20 binding [Leclerc et al., 2005]. The Wnt pathway was stimulated either with recombinant Wnt3A or with LiCl, a GSK3β inhibitor. LiCl-mediated stimulation was assessed after correction for ion effects measured in parallel cultures using KCl.

Activation of the Wnt signaling pathway by LiCl significantly increased transcription from both the OKE_3-147-OC-Luc (Fig. 4B) and the 4 × Egr.syn (Fig. 4D) reporters. Recombinant Wnt3A similarly enhanced activity of these Krox reporters, although the activation of OKE_3-147-OC-Luc by Wnt3A did not reach statistical significance, possibly due to the influence of non-EGR transcription factors on this reporter. Interestingly, stimulation of the Krox reporters occurred only upon activation of the Wnt signaling pathway and not in response to other bone anabolic agents tested. Specifically, PTH(1-34) did not increase transcription from either Krox reporter (Fig. 4B,D), while significantly stimulating transcription from a CREB reporter [Miguel et al., 2005] used as positive control (Fig. 4D, inset). Similarly, BMP2 significantly stimulated its classical reporter, 12 × SBE [Zhao et al., 2003] (Fig. 4D, inset), but not 4 × Egr.syn (Fig. 4D). OKE_3-147-OC-Luc (Fig. 4B) was not stimulated by BMP2 beyond the level observed with the corresponding OKE mutant construct (Fig. 4C), which is attributable to the Runx2 site (see Fig. 4A). Thus, results using both the OKE_3-147-OC-Luc and the 4 × Egr.syn reporters suggest that Krox20 may play a role specifically downstream of the Wnt signaling pathway in osteoblasts. Stimulation of Krox20 activity could be accounted for by the increase in Krox20 mRNA, which was observed already 0.5 h after treatment of MC3T3-E1 cultures with Wnt3A, and became significant at 2 and 4 h (Fig. 4E). Notably, however, the effect of Wnt3A was transient; it was followed by down-regulation of Krox20 mRNA to levels significantly lower than the respective controls, reflecting tight regulation of this gene (Fig. 4E). Altogether, a role for Krox20 in osteoblast function is supported by the following observations: (i) it is up-regulated during terminal osteoblast differentiation (Fig. 1A,C); (ii) it is stimulated by Wnt3A (Fig. 4B–E); (iii) it is repressed by GCs (Figs. 1A,C and 2); (iv) it enhances OC transcription [Leclerc et al., 2005]; and (v) it contributes to embryonic trabecular bone formation [Levi et al., 1996].

Involvement of the Wnt Signaling Pathway in DEX-Mediated Krox20 Repression

We previously reported that GCs inhibit Wnt signaling in osteoblasts [Smith et al., 2002; Smith and Frenkel, 2005]. Because GCs inhibit, and Wnt3A stimulates Krox20 expression ([Leclerc et al., 2004, 2005] and Figs. 1, 2, and 4), we asked whether the repression of Krox20 by GCs is attributable to the inhibition

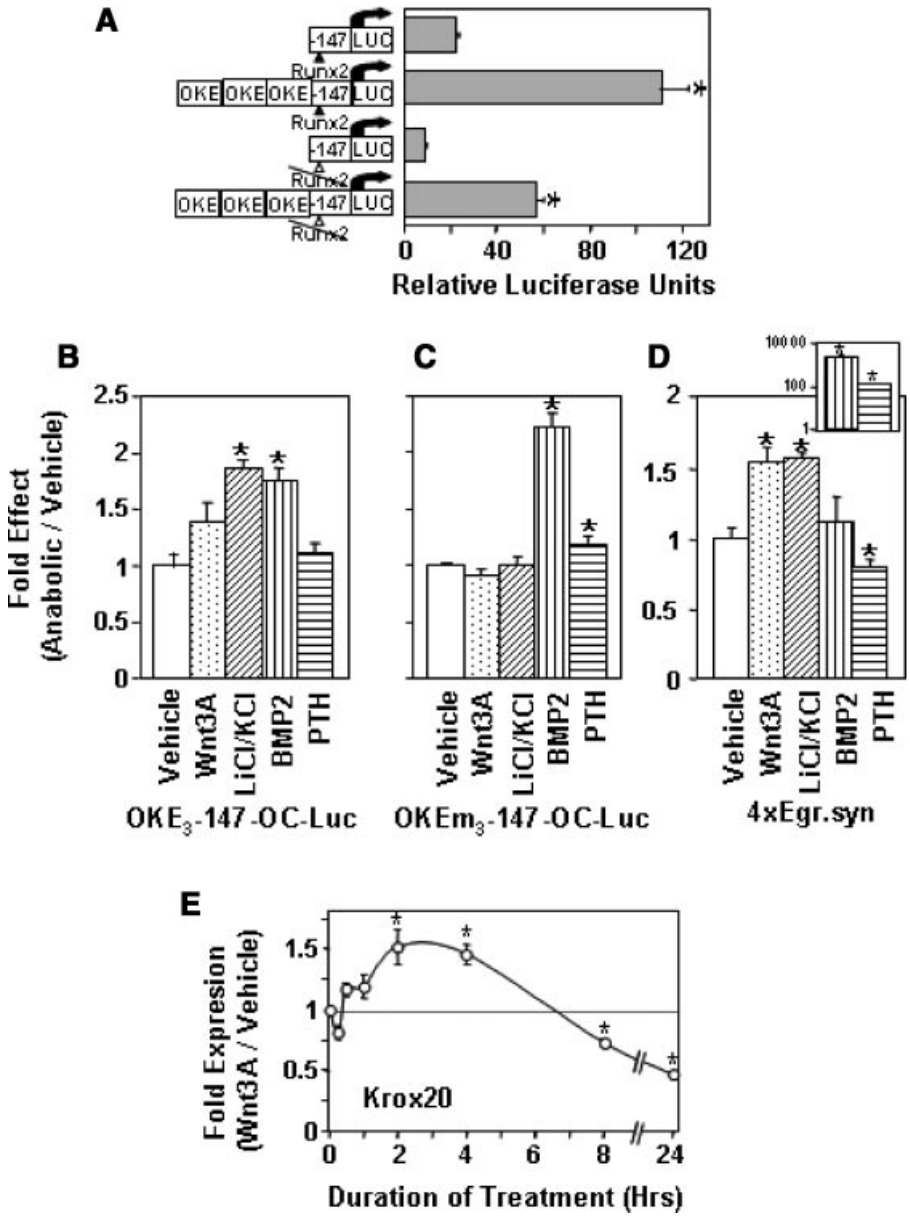

Fig. 4. Wnt stimulates Krox20. **A**: MC3T3-E1 cells were subjected to long-term transient transfection as previously described [Leclerc et al., 2005] and luciferase activity was measured on Day 6. Representative results (mean ± SEM) are shown from one of three independent experiments performed in triplicate wells. The constructs, illustrated on the left, were -147-OC-luc (*top*), OKE_3-147-OC-luc, -147-OC-Runx2m-luc, and OKE_3-147-OC-Runx2m-luc; $^*P \leq 0.05$. **B–D**: MC3T3-E1 cultures were stably (B,C) or transiently (D) transfected with the indicated Krox reporter constructs as described in Materials and Methods Section. On Day 3, cells were treated for 24 h in serum-free medium with either Vehicle, 10 ng/ml rmWnt3A, 40 mM LiCl, 40 mM KCl, 100 ng/ml rhBMP2, and 50 nM PTH(1-34) as indicated. Each bar represents luciferase activity (Mean ± SEM; n = 3) normalized for the mean Vehicle value, which itself is defined as 1. The values measured in the LiCl-treated cultures were corrected for those measured in KCl-treated cultures to account for ion effects. *Inset* in **Panel D** demonstrates the effects of rhBMP2 and PTH(1-34) on their classical response elements, which bind SMAD ($12 \times$ SBE) and CREB (CRE_4-Luc), respectively; $^*P \leq 0.05$. **E**: Krox20 mRNA levels were measured by RT-qPCR in MC3T3-E1 cells untreated or treated with 40 ng/ml rmWnt3A for the indicated time periods. Values were corrected for the expression of rpL10A mRNA, which itself did not respond to treatment. Each data point is the ratio between the value measured in Wnt3A-treated versus the respective control culture (mean ± SEM; n = 3); $^*P \leq 0.05$.

of the Wnt signaling pathway. To this end, we measured the extent of Krox20 inhibition by DEX after activation of the Wnt pathway with Wnt3A and after repression of the pathway with the Wnt antagonist DKK1. When Wnt signaling was activated with Wnt3A, DEX significantly inhibited Krox20 expression by more than six-fold (Fig. 5A). As expected, co-treatment with DKK1 almost completely negated the Wnt3A-mediated activation of the pathway, as evidenced by the prevention of Cyclin D1 up-regulation (Fig. 5B). In the presence of DKK1, Krox20 expression decreased to levels close to those observed in the absence of Wnt3A, and the DEX-mediated repression of Krox20 was reduced from 6-fold to 3.7-fold. Thus, GCs inhibit both the mechanisms driving Krox20 expression in Wnt-deprived cells (presence of DKK1) and the additional mechanisms responsible for augmentation of Krox20 expression by Wnt (Fig. 5C).

Wnt3A Partially Rescues DEX-Inhibited Krox20 Expression and Extracellular Matrix Mineralization

Because the Wnt signaling pathway is involved in GC-mediated inhibition of Krox20 (Fig. 5), and because Krox20 is implicated in osteogenesis ([Levi et al., 1996] and Fig. 1), we asked whether treatment with Wnt3A could antagonize the inhibitory effects of GCs on both Krox20 and the osteoblast phenotype. Initially, we treated MC3T3-E1 cultures for 4 h with DEX, Wnt3A, or both reagents combined. As shown in Figure 6, DEX treatment decreased Krox20 mRNA to 28% of the control level. Co-treatment with Wnt3A partially rescued Krox20 expression up to 46% the control level, which was a significant 68% increase compared to the level measured with DEX alone (Fig. 6). On a side note, shorter treatments with Wnt3A were insufficient to rescue Krox20 expression in the presence of DEX.

We next tested whether Wnt3A could also counteract the inhibitory effect of GCs on the osteoblast phenotype. MC3T3-E1 cultures were chronically treated with DEX, commencing on Day 3, and Wnt3A was co-administered either chronically, between Days 3 and 11, or briefly, for 48-h between Days 3 and 5. Calcium deposition was assessed by alizarin red staining. Whereas chronic Wnt3A treatment did not counteract the inhibitory effect of DEX (Fig. 7A), brief exposure of the GC-treated cultures to Wnt3A rescued mineralization (Fig. 7B). However, microscopic evaluation

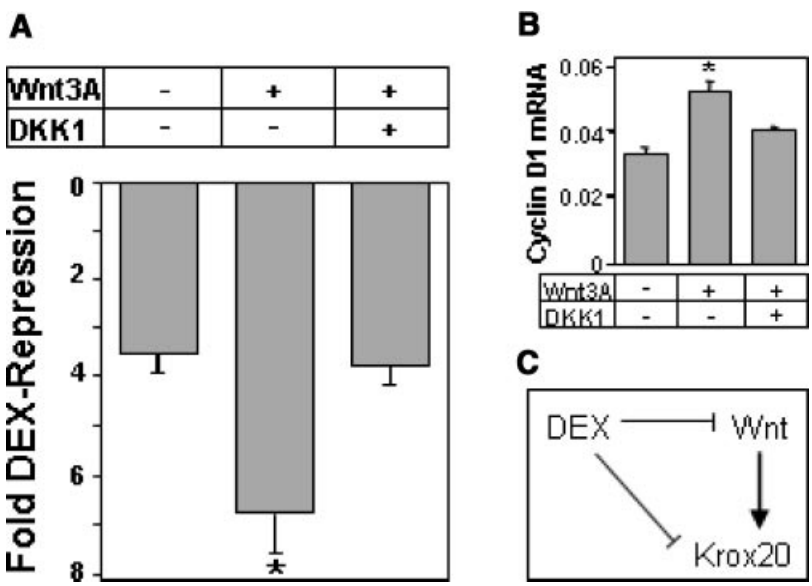

Fig. 5. DEX inhibits Krox20 expression via DKK1-sensitive and -insensitive mechanisms. **A**: MC3T3-E1 cultures were treated for 2.5 h with 1 μM DEX in the presence or absence of 10 ng/ml rmWnt3A alone or in combination with 25 ng/ml rhDKK1. Total mRNA was collected and Krox20 mRNA was measured by RT-qPCR. Data (mean ± SEM) are from one representative of 3 experiments, and are expressed as DEX-mediated fold repression. **B**: Cyclin D1 mRNA was measured by RT-qPCR in the Wnt3A-treated and Wnt3A/DKK1-co-treated cultures to control for the inhibition of Wnt signaling by DKK1. **C**: Schematic illustration describing the dual inhibitory mechanism, direct and indirect, by which GCs inhibit Krox20. $^*P \leq 0.05$ when compared to each of the other two conditions.

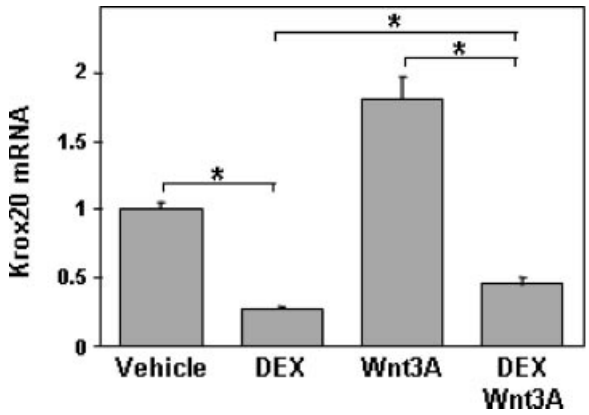

Fig. 6. Wnt3A partially rescues Krox20 expression in DEX-treated cultures. MC3T3-E1 cultures were treated for 4 h with 10 ng/ml rmWnt3A or vehicle in the presence or absence of 1 μM DEX. Total mRNA was collected and Krox20 mRNA was measured by RT-qPCR. Results (mean ± SD, n = 3) are corrected for rpL10A mRNA; $*P \leq 0.05$.

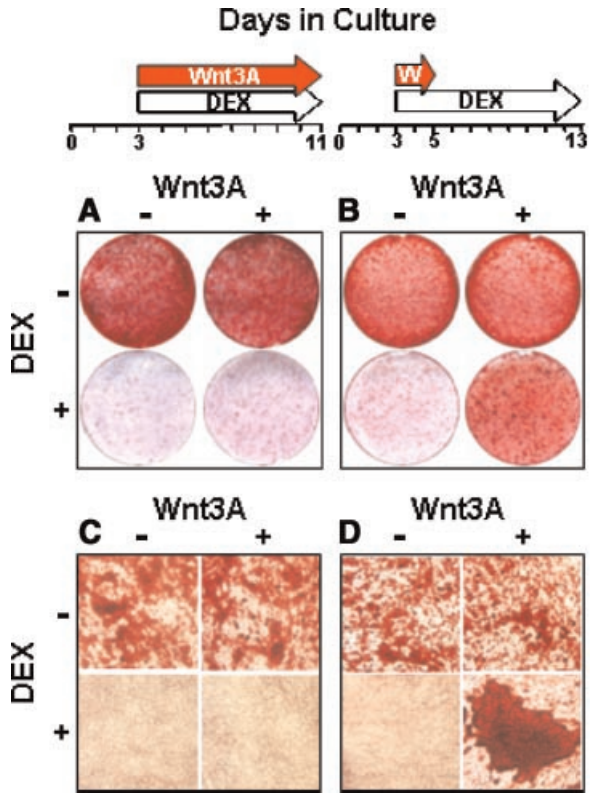

Fig. 7. Wnt3A induces formation of large mineralized nodules in DEX-treated cultures. MC3T3-E1 cultures were treated with 10 ng/ml rmWnt3A or vehicle in the presence or absence of 1 μM DEX commencing on Day 3. **A**,**C**: DEX and Wnt3A were administered chronically, and alizarin red staining was performed on Day 11. **B**,**D**: DEX was chronically administered between Days 3 and 13 and Wnt3A was administered between Day 3 and Day 5. Alizarin red staining was performed on Day 13. **Panels C**,**D** are representative bright-field micrographs (100×) of the cultures scanned in **Panels A**,**B**, respectively. [Color figure can be viewed in the online issue, which is available at www.interscience.wiley.com.]

revealed a clear difference between the mineralization patterns in the control versus the Wnt3A-rescued cultures (Fig. 7D). Whereas the mineralized nodules in the control (and the Wnt3A-treated) cultures were small and abundant, they were fewer but much larger after co-treatment with DEX and Wnt3A, suggesting enhanced development of the osteoblast phenotype in fewer foci as compared to the untreated cultures.

DISCUSSION

While best studied in the context of the nervous system, Krox20 is also expressed elsewhere, including in osteoblasts and chondrocytes [Levi et al., 1996; Voiculescu et al., 2000]. A role for Krox20 in osteogenesis is suggested by the arrest of trabecular bone formation observed in Krox20 knockout mouse embryos [Levi et al., 1996]. Further supporting a role for this gene in osteoblasts, the present study demonstrates regulation of Krox20 by the Wnt signaling pathway, among the most important in controlling osteoblast growth and differentiation (reviewed in Westendorf et al. [2004] and Glass and Karsenty [2006]). These observations suggest that the strong inhibition of Krox20 in response to GCs contributes to glucocorticoid-induced osteoporosis (GIO). Consistent with this notion, we show in the present study that GCs very strongly and rapidly suppress Krox20 expression and that treatment with Wnt3A partially rescues both Krox20 expression and mineralized nodule formation in GC-arrested osteoblast cultures.

EGR transcription factors have been implicated in mediating the mitogenic activities of growth factors [Milbrandt, 1987; Lemaire et al., 1988]. Therefore, the respective positive and negative regulation of Krox20 by Wnt signaling and GCs is likely related to their activities on the osteoblast cell cycle, in particular a uniquely controlled cell cycle that occurs during commitment to the bone phenotype [Smith et al., 2000]. Like Krox20, this cell cycle is inhibited by GCs and rescued by activation of the Wnt signaling pathway [Smith et al., 2002]. Indeed, there is evidence that the so-called differentiation-related cell cycle directly contributes to development of the bone phenotype [Smith et al., 2000].

Such a role for Krox20 in osteoblasts would add to the growing evidence that Krox20 is essential for the specification of various cell lineages including Schwann cells [Topilko et al., 1994; Zorick et al., 1996; Warner et al., 1998], chondrocytes undergoing chondro-osteoblastic transformation [Levi et al., 1996], and adipocytes [Chen et al., 2005]. Further supporting a role for Krox20 in cell type-specific events, activity of the OKE is differentiation-related and dependent on Runx2 expression [Leclerc et al., 2005].

All EGR mRNAs were readily detectable in primary osteoblast cultures, and the four genes displayed similar expression patterns. Initially their levels dropped during early stages of cell proliferation and condensation, likely reflecting down-regulation of cell cycle progression. Thereafter, the EGR mRNAs increased as the cultures started to deposit a bony matrix. Although the late increase in EGR mRNAs suggest that they may play a role in osteoblast differentiation, Krox20-deficient osteoblast cultures deposited mineralized extracellular matrix in a manner undistinguishable from control cultures (data not shown). Possibly, functional redundancy allowed other EGR family members to compensate for the deficiency in Krox20. However, such redundancy would not secure EGR function in the presence of GCs, because GCs strongly suppress all EGR genes. The molecular mechanisms underlying GC-mediated repression may be unique to each of the four EGR genes because alignment of ~100-kb surrounding each gene did not reveal any region with significant homology across the four genes, with the exception of the sequences encoding the DNA-binding domains.

In addition to repression of Krox20 itself, GCs also repressed expression of the Krox20 co-activator HCF-1 more than they did to the EGR co-repressors NAB1, NAB2, and Ddx20. The multi-pronged repression of the EGR network may participate in all or some of the deleterious skeletal effects of GCs. These include: (1) inhibition of pre-osteoblast proliferation, as EGRs are classically implicated in cell growth [Milbrandt, 1987; Christy et al., 1988; Lemaire et al., 1988]; (2) impairment of osteoblast differentiation, as EGRs have been implicated in cellular specification [Topilko et al., 1994; Levi et al., 1996; Zorick et al., 1996; Warner et al., 1998; Chen et al., 2005]; (3) attenuation of α1(I) collagen synthesis, as c-Krox, a relative of the EGR family, has been implicated in this promoter's activity [Galera et al., 1994; Galera et al., 1996]; (4) promotion of apoptosis [Zalavras et al., 2003; O'Brien et al., 2004], as EGRs have been implicated in the control of cell survival [Tourtellotte et al., 1999; Thiel and Cibelli, 2002; Parkinson et al., 2004]; and (5) stimulation of bone resorption [Jia et al., 2006; Kim et al., 2006], as mice lacking EGR1 display high bone turnover and low bone mass [Cenci et al., 2000].

Multiple signal transduction pathways are necessary for development of the osteoblast phenotype, and many of them are abrogated by GCs. Besides Wnt, these include the FGF, IGF, Notch, and the BMP signaling pathways [Delany et al., 2001; Pereira et al., 2002; Luppen et al., 2003a,b; Leclerc et al., 2004]. Several recent studies focused on GC-mediated inhibition of the Wnt signaling pathway, which occurs via GSK3β activation [Smith et al., 2002], GSK3β-independent inhibition of LEF/TCF activity [Smith and Frenkel, 2005], and stimulation of the Wnt antagonists DKK1 [Ohnaka et al., 2004] and sFRP-1 [Wang et al., 2005]. The variety of mechanisms by which GCs adversely affect the skeleton renders the task of GIO treatment extremely difficult. Administration of recombinant BMP2 restores mineralization in GC-arrested osteoblast cultures but does not rescue Krox20 expression (data not shown) or collagen accumulation [Luppen et al., 2003a,b]. In the present study we show that the partial rescue of Krox20 by recombinant Wnt3A is associated with partial rescue of mineralization in focal but highly developed bony nodules. It will be interesting to see whether co-treatment of GC-arrested cultures with both BMPs and Wnts results in a more complete rescue. Such an approach, however, must take into consideration that, unlike BMP2, which delivers positive results whether administered acutely [Luppen et al., 2003a] or chronically [Luppen et al., 2003b], Wnt3A must be administered for only a short period of time. The negative outcome of chronic administration (Fig. 7A) possibly reflects the requirement for down-regulation of the Wnt signaling pathway at very late stages of osteoblast differentiation [de Boer et al., 2004; Li et al., 2005; van der Horst et al., 2005], although such requirement in the present study was only apparent in the presence of DEX (Fig. 7). Interestingly, mineralization was not perturbed by prolonged Wnt

treatment in the absence of DEX (Fig. 7). Possibly, the rescued mineralization in the DEX/Wnt3A co-treated cultures occurred via molecular mechanisms different from those operative in control cultures. Such notion is supported by the different morphology of the mineralized nodules under the two conditions.

In summary, we show that GCs rapidly inhibit expression of all four EGR genes. The inhibition of Krox20 is mediated, at least in part, by a direct, CHX-resistant mechanism, and is attributable in part to the inhibition of the Wnt signaling pathway. Recombinant Wnt3A partially rescues both Krox20 expression and mineralized nodule formation, advocating the development of therapies for GIO that take advantage of the anti-GC activities of Wnts.

ACKNOWLEDGMENTS

We thank Drs. Gerard Karsenty (Columbia University Medical Center), John Svaren (Vanderbilt University), Stephen Harris (University of Texas Health Science Center at San Antonio) and Michael Chorev (Beth Israel Deaconess Medical Center) for reporter plasmids. rhBMP2 was a generous gift from Wyeth Pharmaceuticals (Cambridge, MA). This study was supported by grants from the Arthritis Foundation (Atlanta, Georgia) and the NIH (AR047052), and by the J. Harold and Edna L. LaBriola Chair in Genetic Orthopaedic Research at the University of Southern California (held by BF). The experiments were conducted in a facility constructed with support from Research Facilities Improvement Program Grant Number C06 (RR10600-01, CA62528-01, RR14514-01) from the NIH/NCRR.

REFERENCES

Babij P, Zhao W, Small C, Kharode Y, Yaworsky PJ, Bouxsein ML, Reddy PS, Bodine PV, Robinson JA, Bhat B, Marzolf J, Moran RA, Bex F. 2003. High bone mass in mice expressing a mutant LRP5 gene. J Bone Miner Res 18:960–974.

Banerjee C, Hiebert SW, Stein JL, Lian JB, Stein GS. 1996. An AML-1 consensus sequence binds an osteoblast-specific complex and transcriptionally activates the osteocalcin gene. Proc Natl Acad Sci USA 93:4968–4973.

Boyden LM, Mao J, Belsky J, Mitzner L, Farhi A, Mitnick MA, Wu D, Insogna K, Lifton RP. 2002. High bone density due to a mutation in LDL-receptor-related protein 5. N Engl J Med 346:1513–1521.

Canalis E. 2005. Mechanisms of glucocorticoid action in bone. Curr Osteoporos Rep 3:98–102.

Cenci S, Weitzmann MN, Gentile MA, Aisa MC, Pacifici R. 2000. M-CSF neutralization and egr-1 deficiency prevent ovariectomy-induced bone loss. J Clin Invest 105:1279–1287.

Chavrier P, Zerial M, Lemaire P, Almendral J, Bravo R, Charnay P. 1988. A gene encoding a protein with zinc fingers is activated during G0/G1 transition in cultured cells. EMBO J 7:29–35.

Chavrier P, Vesque C, Galliot B, Vigneron M, Dolle P, Duboule D, Charnay P. 1990. The segment-specific gene Krox-20 encodes a transcription factor with binding sites in the promoter region of the Hox-1.4 gene. EMBO J 9: 1209–1218.

Chen Z, Torrens JI, Anand A, Spiegelman BM, Friedman JM. 2005. Krox20 stimulates adipogenesis via C/EBP-beta-dependent and -independent mechanisms. Cell Metab 1:93–106.

Christy BA, Lau LF, Nathans D. 1988. A gene activated in mouse 3T3 cells by serum growth factors encodes a protein with "zinc finger" sequences. Proc Natl Acad Sci USA 85:7857–7861.

de Boer J, Siddappa R, Gaspar C, van Apeldoorn A, Fodde R, van Blitterswijk C. 2004. Wnt signaling inhibits osteogenic differentiation of human mesenchymal stem cells. Bone 34:818–826.

Delany AM, Durant D, Canalis E. 2001. Glucocorticoid suppression of IGF I transcription in osteoblasts. Mol Endocrinol 15:1781–1789.

Ducy P, Karsenty G. 1995. Two distinct osteoblast-specific cis-acting elements control expression of a mouse osteocalcin gene. Mol Cell Biol 15:1858–1869.

Fang MA, Noguchi GM, McDougall S. 1996. Prostaglandin E2 induces Egr-1 mRNA in MC3T3-E1 osteoblastic cells by a protein kinase C-dependent pathway. Prostaglandins Leukot Essent Fatty Acids 54:109–114.

Frenkel B, Montecino M, Green J, Aslam F, Desai R, Banerjee C, Stein JL, Lian JB, Stein GS. 1996. Basal and vitamin D-responsive activity of the rat osteocalcin promoter in stably transfected osteosarcoma cells: Requirement of upstream sequences for control by the proximal regulatory domain. Endocrinology 137:1080–1088.

Galera P, Musso M, Ducy P, Karsenty G. 1994. c-Krox, a transcriptional regulator of type I collagen gene expression, is preferentially expressed in skin. Proc Natl Acad Sci USA 91:9372–9376.

Galera P, Park RW, Ducy P, Mattei MG, Karsenty G. 1996. c-Krox binds to several sites in the promoter of both mouse type I collagen genes. Structure/function study and developmental expression analysis. J Biol Chem 271: 21331–21339.

Gashler A, Sukhatme VP. 1995. Early growth response protein 1 (Egr-1): Prototype of a zinc-finger family of transcription factors. Prog Nucleic Acid Res Mol Biol 50: 191–224.

Gillian AL, Svaren J. 2004. The Ddx20/DP103 dead box protein represses transcriptional activation by Egr2/Krox-20. J Biol Chem 279:9056–9063.

Glass DA 2nd, Karsenty G. 2006. Molecular bases of the regulation of bone remodeling by the canonical Wnt signaling pathway. Curr Top Dev Biol 73:43–84.

Gong Y, Slee RB, Fukai N, Rawadi G, Roman-Roman S, Reginato AM, Wang H, Cundy T, Glorieux FH, Lev D, Zacharin M, Oexle K, Marcelino J, Suwairi W, Heeger S,

Sabatakos G, Apte S, Adkins WN, Allgrove J, Arslan-Kirchner M, Batch JA, Beighton P, Black GC, Boles RG, Boon LM, Borrone C, Brunner HG, Carle GF, Dallapiccola B, De Paepe A, Floege B, Halfhide ML, Hall B, Hennekam RC, Hirose T, Jans A, Juppner H, Kim CA, Keppler-Noreuil K, Kohlschuetter A, LaCombe D, Lambert M, Lemyre E, Letteboer T, Peltonen L, Ramesar RS, Romanengo M, Somer H, Steichen-Gersdorf E, Steinmann B, Sullivan B, Superti-Furga A, Swoboda W, van den Boogaard MJ, Van Hul W, Vikkula M, Votruba M, Zabel B, Garcia T, Baron R, Olsen BR, Warman ML. 2001. LDL receptor-related protein 5 (LRP5) affects bone accrual and eye development. Cell 107:513–523.

Hass R, Brach M, Gunji H, Kharbanda S, Kufe D. 1992. Inhibition of EGR-1 and NF-kappa B gene expression by dexamethasone during phorbol ester-induced human monocytic differentiation. Biochem Pharmacol 44:1569–1576.

Jia D, O'Brien CA, Stewart SA, Manolagas SC, Weinstein RS. 2006. Glucocorticoids act directly on osteoclasts to increase their life span and reduce bone density. Endocrinology 147:5592–5599.

Kato M, Patel MS, Levasseur R, Lobov I, Chang BH, Glass DA II, Hartmann C, Li L, Hwang TH, Brayton CF, Lang RA, Karsenty G, Chan L. 2002. Cbfa1-independent decrease in osteoblast proliferation, osteopenia, and persistent embryonic eye vascularization in mice deficient in Lrp5, a Wnt coreceptor. J Cell Biol 157:303–314.

Kharbanda S, Nakamura T, Stone R, Hass R, Bernstein S, Datta R, Sukhatme VP, Kufe D. 1991. Expression of the early growth response 1 and 2 zinc finger genes during induction of monocytic differentiation. J Clin Invest 88: 571–577.

Kim HJ, Zhao H, Kitaura H, Bhattacharyya S, Brewer JA, Muglia LJ, Ross FP, Teitelbaum SL. 2006. Glucocorticoids suppress bone formation via the osteoclast. J Clin Invest 116:2152–2160.

Leclerc N, Luppen CA, Ho VV, Nagpal S, Hacia JG, Smith E, Frenkel B. 2004. Gene expression profiling of glucocorticoid-inhibited osteoblasts. J Mol Endocrinol 33:175–193.

Leclerc N, Noh T, Khokhar A, Smith E, Frenkel B. 2005. Glucocorticoids inhibit osteocalcin transcription in osteoblasts by suppressing Egr2/Krox20-binding enhancer. Arthritis Rheum 52:929–939.

Lee SL, Sadovsky Y, Swirnoff AH, Polish JA, Goda P, Gavrilina G, Milbrandt J. 1996. Luteinizing hormone deficiency and female infertility in mice lacking the transcription factor NGFI-A (Egr-1). Science 273:1219–1221.

Lemaire P, Revelant O, Bravo R, Charnay P. 1988. Two mouse genes encoding potential transcription factors with identical DNA-binding domains are activated by growth factors in cultured cells. Proc Natl Acad Sci USA 85:4691–4695.

Levi G, Topilko P, Schneider-Maunoury S, Lasagna M, Mantero S, Cancedda R, Charnay P. 1996. Defective bone formation in Krox-20 mutant mice. Development 122: 113–120.

Li X, Liu P, Liu W, Maye P, Zhang J, Zhang Y, Hurley M, Guo C, Boskey A, Sun L, Harris SE, Rowe DW, Ke HZ, Wu D. 2005. Dkk2 has a role in terminal osteoblast differentiation and mineralized matrix formation. Nat Genet 37:945–952.

Little RD, Carulli JP, Del Mastro RG, Dupuis J, Osborne M, Folz C, Manning SP, Swain PM, Zhao SC, Eustace B, Lappe MM, Spitzer L, Zweier S, Braunschweiger K, Benchekroun Y, Hu X, Adair R, Chee L, FitzGerald MG, Tulig C, Caruso A, Tzellas N, Bawa A, Franklin B, McGuire S, Nogues X, Gong G, Allen KM, Anisowicz A, Morales AJ, Lomedico PT, Recker SM, Van Eerdewegh P, Recker RR, Johnson ML. 2002. A mutation in the LDL receptor-related protein 5 gene results in the autosomal dominant high-bone-mass trait. Am J Hum Genet 70: 11–19.

Luciano RL, Wilson AC. 2003. HCF-1 functions as a coactivator for the zinc finger protein Krox20. J Biol Chem 278:51116–51124.

Luppen CA, Leclerc N, Noh T, Barski A, Khokhar A, Boskey AL, Smith E, Frenkel B. 2003a. Brief bone morphogenetic protein 2 treatment of glucocorticoid-inhibited MC3T3-E1 osteoblasts rescues commitment-associated cell cycle and mineralization without alteration of Runx2. J Biol Chem 278:44995–45003.

Luppen CA, Smith E, Spevak L, Boskey AL, Frenkel B. 2003b. Bone morphogenetic protein-2 restores mineralization in glucocorticoid-inhibited MC3T3-E1 osteoblast cultures. J Bone Miner Res 18:1186–1197.

Mazziotti G, Angeli A, Bilezikian JP, Canalis E, Giustina A. 2006. Glucocorticoid-induced osteoporosis: An update. Trends Endocrinol Metab 17:144–149.

Miguel SM, Namdar-Attar M, Noh T, Frenkel B, Bab I. 2005. ERK1/2-activated de novo Mapkapk2 synthesis is essential for osteogenic growth peptide mitogenic signaling in osteoblastic cells. J Biol Chem 280:37495–37502.

Milbrandt J. 1987. A nerve growth factor-induced gene encodes a possible transcriptional regulatory factor. Science 238:797–799.

Mittelstadt PR, Ashwell JD. 2001. Inhibition of AP-1 by the glucocorticoid-inducible protein GILZ. J Biol Chem 276: 29603–29610.

Molnar G, Crozat A, Pardee AB. 1994. The immediate-early gene Egr-1 regulates the activity of the thymidine kinase promoter at the G0-to-G1 transition of the cell cycle. Mol Cell Biol 14:5242–5248.

Nonchev S, Maconochie M, Vesque C, Aparicio S, Ariza-McNaughton L, Manzanares M, Maruthainar K, Kuroiwa A, Brenner S, Charnay P, Krumlauf R. 1996. The conserved role of Krox-20 in directing Hox gene expression during vertebrate hindbrain segmentation. Proc Natl Acad Sci USA 93:9339–9345.

O'Brien CA, Jia D, Plotkin LI, Bellido T, Powers CC, Stewart SA, Manolagas SC, Weinstein RS. 2004. Glucocorticoids act directly on osteoblasts and osteocytes to induce their apoptosis and reduce bone formation and strength. Endocrinology 145:1835–1841.

O'Donovan KJ, Tourtellotte WG, Millbrandt J, Baraban JM. 1999. The EGR family of transcription-regulatory factors: Progress at the interface of molecular and systems neuroscience. Trends Neurosci 22:167–173.

Ohnaka K, Taniguchi H, Kawate H, Nawata H, Takayanagi R. 2004. Glucocorticoid enhances the expression of dickkopf-1 in human osteoblasts: Novel mechanism of glucocorticoid-induced osteoporosis. Biochem Biophys Res Commun 318:259–264.

Ohnaka K, Tanabe M, Kawate H, Nawata H, Takayanagi R. 2005. Glucocorticoid suppresses the canonical Wnt

signal in cultured human osteoblasts. Biochem Biophys Res Commun 329:177–181.

Parkinson DB, Bhaskaran A, Droggiti A, Dickinson S, D'Antonio M, Mirsky R, Jessen KR. 2004. Krox-20 inhibits Jun-NH2-terminal kinase/c-Jun to control Schwann cell proliferation and death. J Cell Biol 164: 385–394.

Pereira RM, Delany AM, Durant D, Canalis E. 2002. Cortisol regulates the expression of Notch in osteoblasts. J Cell Biochem 85:252–258.

Petersohn D, Schoch S, Brinkmann DR, Thiel G. 1995. The human synapsin II gene promoter. Possible role for the transcription factor zif268/egr-1, polyoma enhancer activator 3, and AP2. J Biol Chem 270:24361–24369.

Russo MW, Sevetson BR, Milbrandt J. 1995. Identification of NAB1, a repressor of NGFI-A- and Krox20-mediated transcription. Proc Natl Acad Sci USA 92:6873–6877.

Schneider-Maunoury S, Topilko P, Seitandou T, Levi G, Cohen-Tannoudji M, Pournin S, Babinet C, Charnay P. 1993. Disruption of Krox-20 results in alteration of rhombomeres 3 and 5 in the developing hindbrain. Cell 75:1199–1214.

Smith E, Frenkel B. 2005. Glucocorticoids inhibit the transcriptional activity of LEF/TCF in differentiating osteoblasts in a glycogen synthase kinase-3beta-dependent and -independent manner. J Biol Chem 280:2388–2394.

Smith E, Redman RA, Logg CR, Coetzee GA, Kasahara N, Frenkel B. 2000. Glucocorticoids inhibit developmental stage-specific osteoblast cell cycle. Dissociation of cyclin A-cyclin-dependent kinase 2 from E2F4-p130 complexes. J Biol Chem 275:19992–20001.

Smith E, Coetzee GA, Frenkel B. 2002. Glucocorticoids inhibit cell cycle progression in differentiating osteoblasts via glycogen synthase kinase-3beta. J Biol Chem 277:18191–18197.

Suva LJ, Ernst M, Rodan GA. 1991. Retinoic acid increases zif268 early gene expression in rat preosteoblastic cells. Mol Cell Biol 11:2503–2510.

Svaren J, Sevetson BR, Apel ED, Zimonjic DB, Popescu NC, Milbrandt J. 1996. NAB2, a corepressor of NGFI-A (Egr-1) and Krox20, is induced by proliferative and differentiative stimuli. Mol Cell Biol 16:3545–3553.

Swirnoff AH, Milbrandt J. 1995. DNA-binding specificity of NGFI-A and related zinc finger transcription factors. Mol Cell Biol 15:2275–2287.

Thiel G, Cibelli G. 2002. Regulation of life and death by the zinc finger transcription factor Egr-1. J Cell Physiol 193: 287–292.

Topilko P, Schneider-Maunoury S, Levi G, Baron-Van Evercooren A, Chennoufi AB, Seitanidou T, Babinet C, Charnay P. 1994. Krox-20 controls myelination in the peripheral nervous system. Nature 371:796–799.

Topilko P, Schneider-Maunoury S, Levi G, Trembleau A, Gourdji D, Driancourt MA, Rao CV, Charnay P. 1998. Multiple pituitary and ovarian defects in Krox-24 (NGFI-A, Egr-1)-targeted mice. Mol Endocrinol 12:107–122.

Tourtellotte WG, Milbrandt J. 1998. Sensory ataxia and muscle spindle agenesis in mice lacking the transcription factor Egr3. Nat Genet 20:87–91.

Tourtellotte WG, Nagarajan R, Auyeung A, Mueller C, Milbrandt J. 1999. Infertility associated with incomplete spermatogenic arrest and oligozoospermia in Egr4-deficient mice. Development 126:5061–5071.

van der Horst G, van der Werf SM, Farih-Sips H, van Bezooijen RL, Lowik CW, Karperien M. 2005. Downregulation of Wnt signaling by increased expression of Dickkopf-1 and -2 is a prerequisite for late-stage osteoblast differentiation of KS483 cells. J Bone Miner Res 20:1867–1877.

Van Staa TP, Leufkens HG, Abenhaim L, Zhang B, Cooper C. 2000. Use of oral corticosteroids and risk of fractures. J Bone Miner Res 15:993–1000.

Voiculescu O, Charnay P, Schneider-Maunoury S. 2000. Expression pattern of a Krox-20/Cre knock-in allele in the developing hindbrain, bones, and peripheral nervous system. Genesis 26:123–126.

Wang FS, Lin CL, Chen YJ, Wang CJ, Yang KD, Huang YT, Sun YC, Huang HC. 2005. Secreted frizzled-related protein 1 modulates glucocorticoid attenuation of osteogenic activities and bone mass. Endocrinology 146:2415–2423.

Warner LE, Mancias P, Butler IJ, McDonald CM, Keppen L, Koob KG, Lupski JR. 1998. Mutations in the early growth response 2 (EGR2) gene are associated with hereditary myelinopathies. Nat Genet 18:382–384.

Westendorf JJ, Kahler RA, Schroeder TM. 2004. Wnt signaling in osteoblasts and bone diseases. Gene 341:19–39.

Wilkinson DG, Bhatt S, Chavrier P, Bravo R, Charnay P. 1989. Segment-specific expression of a zinc-finger gene in the developing nervous system of the mouse. Nature 337: 461–464.

Zalavras C, Shah S, Birnbaum MJ, Frenkel B. 2003. Role of apoptosis in glucocorticoid-induced osteoporosis and osteonecrosis. Crit Rev Eukaryot Gene Expr 13:221–235.

Zhao M, Qiao M, Oyajobi BO, Mundy GR, Chen D. 2003. E3 ubiquitin ligase Smurf1 mediates core-binding factor alpha1/Runx2 degradation and plays a specific role in osteoblast differentiation. J Biol Chem 278:27939–27944.

Zorick TS, Syroid DE, Arroyo E, Scherer SS, Lemke G. 1996. The transcription factors SCIP and Krox-20 mark distinct stages and cell fates in Schwann cell differentiation. Mol Cell Neurosci 8:129–145.